The Intramolecular Electronic Interaction Regulated by Five-membered Heterocycle Spacer

Yuqiang Hu
Inner Mongolia University of Technology
Limin Han
Inner Mongolia University of Technology
Na Wang (wangna_lisa@126.com)
Baotou Teachers' College

Research Article

Keywords: diferrocenyl derivatives, intramolecular electronic interaction properties, central heterocycle spacer species

Posted Date: March 8th, 2021

DOI: https://doi.org/10.21203/rs.3.rs-283721/v1

Abstract

The spacer in diferrocenyl derivatives has significant effects on intramolecular electronic interaction properties. In this work, nine diferrocenyl five-membered heterocyclic molecules are synthesized as models to investigate the effect of intramolecular electron-transfer properties systematically, including 2,5-diferrocenyl-1-phenyl-pyrrole (**1**), 2,5-diferrocenylfuran (**2**), 2,5-diferrocenylthiophene (**3**), 2,5-diferrocenyl-1H-imidazole (**4**), 2,5-diferrocenyloxazole (**5**), 2,5-diferrocenylthiazole (**6**), 2,5-diferrocenyl-1,3,4-triazole (**7**), 2,5-diferrocenyl-1,3,4-oxadiazole (**8**) and 2,5-diferrocenyl-1,3,4-thiadiazole (**9**). The molecules were prepared in cyclization reaction and characterized by Elemental analysis, FT-IR, MS and NMR. Moreover, the molecular structures of 2,5-diferrocenylthiazole and 2,5-diferrocenyl-1,3,4-oxadiazole were determined by the single crystal X-ray diffraction. The intramolecular electronic interactions were investigated through cyclic voltammetry in combination with density functional theory (DFT) calculations. The results revealed that the electronic interaction decreased with the increase of heteroatoms in central heterocycle spacer, and the electron-transfer property could be regulated by regulate central heterocycle spacer species.

Introduction

The ferrocene (Fc) is widely used in investigating the intramolecular electron transfers due to its redox activity and electrochemical stability, and the research on intramolecular electron transfers could provide simple and convenient for designing prospective ferrocene-containing molecular wires and conducting polymers[1-4]. Generally, two or more ferrocenyl units assembled through various conducting spacers to construct molecular models for studying intramolecular electron transfers[5], the various kind spacers involving of the atom[6], alkenyl[7], alkynyl[8] and various aromatic rings[9]. When one of ferrocene unit occur electrochemical oxidize, an intramolecular donor-acceptor system is formed, the charge may be transfer to the other ferrocene units through the spacers, and the spacers' types[10], structures[11] and chemical properties[12] can influence the electron transfers capability. For example, when a single C atom spacer[13] or a single N atom spacer[14] link two-ferrocene units, the charge transfer capability of the C atom is better than that of the N atom. In addition, diferrocenyl derivatives containing π-conjugate spacers such as the alkenyl[15] and alkynyl[8], the electronic interaction capability of the alkenyl is better than that of the alkynyl. These electronic interaction properties can be associated with the atomic outer boundaries, ionization degree, and hybridization structure factors[16-18]. However, when diferrocenyl derivatives containing aromatic rings spacers, the charge transfers are influenced by various complex factors, including metal-metal center distance[19], position of substituent[20], center ring geometric properties[21], topology[22] and aromatic properties[23,24], which influencing factor is the primary factor of intramolecular electron transfer is still an academic debate. In order to further explore this problem, more and more researchers are engaged in numerous heterocycle spacers' studies, especially the five-membered aromatic heterocycle spacers[25,26], because these spacers involves π-conjugate structure and heteroatom, which can provide changing chemical structure for studying.

In our research group previous works, the spacers' charge density, properties of substituent and coplanarity of block connections were identified as key factors of intramolecular electron-transfers[27-30]. In recent work, the single-heteroatom-five-membered-heterocycle bridged diferrocenyl derivatives were examined, which exhibited the charge transfer highly depend on the short-range heteroatom bridge[31,32], but this research had not systematically accomplished. One of inadequacies was the charge transfer properties on the central five-membered heterocycle spacer containing two and more heteroatoms were still unknown.

To reply the above-mentioned problem, a series of 2,5-diferrocenyl imidazole, oxazole, thiazole, triazole, oxadiazole and thiadiazole derivatives were synthesized as model molecules in this paper (Figure 1), and the intramolecular electron-transfers processes of these model molecules were systematically studied through cyclic voltammetry (CV) and density functional theory (DFT) calculations. The result revealed that the species and the numbers of heteroatom in central spacers could regulate intramolecular electronic transfer processes.

Results And Discussion

The molecular structures and the corresponding data of **1-3** are referenced form our academic paper[31]. The **4-9** were confirmed by FT-IR, ^{1}H-NMR, ^{13}C-NMR, Elemental analysis, and MS (corresponding data are given in synthetic methods). The molecular structure of **6** and **8** were determined by single-crystal X-ray diffraction and shown in Figure S1 and Figure S2. Crystal data and relevant structural parameters enumerate in Table S1. The selected bond lengths, the selected angles and the selected torsion angles list in Table S2 and Table S3. The molecular structure of **9** is referenced form Heinrich Lang published academic paper[33].

Electrochemistry

The redox potential of compounds **1-9** is determined through cyclic voltammetry, and the electrochemical data is listed in Table 1. The compounds **1-6**, **8** and **9** display two redox well-resolved waves in the range of 0-0.8 V (Figure 2-4), which are assigned to the two FeII/FeIII redox couples, from the Ipa/Ipc (≈1) values of each couple, it can be concluded that the redox processes are electrochemical reversible one-electron-transfer processes[31]. The **7** as an exceptional case display one redox well-resolved wave (Figure 2), and it is electrochemical reversible two-electron-transfer process[32].

The first oxidation potentials (Ea_1) of ferrocenyl unit in **1-9** increase, with the increase of heteroatoms in central five-membered heterocycle spacer (Table 1). The Ea_1 of **1** is 58 mV and the Ea_1 of **4** is 138 mV, the Ea_1 of **7** even increase to 344 mV, with the central heterocycle form pyrrole change into imidazole and triazole. The Ea_1 of **2**, **5** and **8** are 184 mV, 328 mV and 321 mV, respectively, the central heterocycle form furan change into oxazole and oxadiazole. The Ea_1 of **3**, **6** and **9** are 217 mV, 304 mV and 308 mV, respectively, the central spacer form thiophene change into thiazole and thiadiazole. The π-conjugation

effects of **3**, **6** and **9** were investigated through comparing the dihedral angles to explore the Ea_1 changing trend. The two dihedral angles formed by cyclopentadiene planes to the central thiophene plane both are 8.93° of **3**. The two dihedral angles formed by cyclopentadiene planes to the central thiazole plane of **6** are different, the one formed by plane S1-C6-N1-C7-C8 to C1-C2-C3-C4-C5 is 3.52°, the other formed by plane S1-C6-N1-C7-C8 to C9-C10-C16-C17-C18 is 5.30°. The two dihedral angles formed by cyclopentadiene planes to the central thiadiazole plane both are 17.08° of **9** (Figure S3). In theory, the smaller dihedral angle indicate more coplanarity between the cyclopentadienyl planes and the central plane, which suggests there are stronger π-conjugation effects with each other, and the Ea_1 should be lower[32]. Hence, the π-conjugation effect order is **6** > **3** > **9** indicate by dihedral angles, the order of Ea_1 should be **6** (Ea_1=304 mV) < **3** (Ea_1=217 mV) < **9** (Ea_1=308 mV), but this result was disagreement with our experiment. Therefore, the embedded N atoms in **6** and **9** debase charge density of central heterocycle with its stronger electron withdrawing effects, and block the charge transfer between two ferrocenyl units.

The electronic communication effects of **1-9** were discussed through comparing the oxidation potential differences (ΔE) with two ferrocenyl units. The ΔE of **1** is 315 mV, the ΔE of **4** is 210 mV. However, the **7** has only one redox wave, of which ΔE cannot be measured. The ΔE of **2** is 161 mV, the ΔE of **5** is 130 mV and the ΔE of **8** is 88 mV. Moreover, the ΔE of **3** is 139 mV, the ΔE of **6** is 124 mV and the ΔE of **9** is 86 mV (Table 1), respectively. Clearly, the values of ΔE are trending downward obviously, which exhibit the embedded N atoms in central spacers have debased electronic communication between two ferrocenyl units.

In general, the shorter distance of bimetal center indicated stronger electrostatic interaction and express larger ΔE[19,31]. However, the order of Fe1-Fe2 distance is **1** (8.518 Å)> **6** (8.420 Å) > **9** (8.047 Å) > **3** (7.084 Å)> **2** (6.599 Å) > **8** (6.581 Å) measured from crystal structure (Figure S4), which is disagreement with the ΔE variation trend **9** (86 mV) < **8** (88 mV) < **6** (124 mV) < **3** (139 mV) < **2** (161 mV) <**1** (315 mV) in our experiment. Hence, the electronic communication of **1-9** is not affected by the Fe-Fe distance.

The π-conjugation effect of ΔE was discussed by crystal structure data. The torsion angles Fe1-C1-C11-O1 (-80.05°) and Fe1'-C1'-C11'-O1 (80.05°) of **2**[31] are bigger than torsion angles O1-C13-14-Fe1 (-66.93°) and O1-C12-C9-Fe2 (73.20°) of **8** (Table S3), which express the π-conjugation effect of diferrocenyl and central spacer is stronger in **2** than in **8**, the electronic communication is stronger in **2** (ΔE=161 mV) than in **8** (ΔE=88 mV). In theory, the stronger π-conjugation effects indicate the better electronic communication between two ferrocenyl units[32]. However, the π-conjugation effect deduced by torsion angles is **6** (Table S3) > **3**[31] > **9**[33], the electronic communication order should be **6** (ΔE=124 mV) > **3** (ΔE=139 mV) > **9** (ΔE=86 mV), but this result is not inagreement with our experiment, which indicates the embedded N atoms in central spacer is more important than π-conjugation effect for electronic communication.

NMR studies confirmed that the aromaticity of central spacers not affect electronic communication. The *β*-H chemical shifts of **1-6** are 6.383 ppm, 6.152 ppm, 6.806 ppm, 7.272 ppm, 6.941 ppm and 7.523 ppm

(Figure S5-S10), respectively. Hence, the aromaticity order of centre heterocycle is **6** > **4** > **5** > **3** > **1** > **2**. In theory, the central spacer bridge has stronger aromatic properties, and there is more strongly intermetallic electron transfer interaction[35,36]. The order of ΔE value should be **6** > **4** > **5** > **3** > **1** > **2** according to aromaticity. However, this result is also not consistent with experiment. Furthermore, the NMR studies cannot be used in confirming the aromaticity of **7**, **8** and **9**, because there have no C-H bonds in central heterocycle. Consequently, the central spacers' aromaticity confirmed by using the Nucleus Independent Chemical Shifts (NICS)[37,38]. The NICS are -14.7369, -14.0069, -14.0642, -12.6821, -12.1474, -11.5493, -19.8319, -19.6180 and -20.4250 corresponding to pyrrole, imidazole, triazole, furan, oxazole, oxadiazole, thiophene, thiazole and thiadiazole, respectively. Hence, the aromaticity order is thiadiazole > thiophene > thiazole > pyrrole > triazole > imidazole > furan > oxazole > oxadiazole, and the ΔE order should be **9** > **3** > **6** > **1** > **7** > **4** > **2** > **5** > **8** deduce by NICS. However, it is not consistent with the ΔE variation trend **7** (none ΔE) < **9** (86 mV) < **8** (88 mV) < **6** (124 mV) < **5** (130 mV) < **3** (139 mV) < **2** (161 mV) < **4** (210 mV) < **1** (315 mV) in this work (Table 1). The NMR and NICS studies confirm that the aromaticity of the central spacers not affect the electronic communication.

The Natural Bond Orbital charge (NBO charge) population of heteroatom studies confirmed that electronic communication was highly affected by shorter heteroatom-linked bridge (Table 2). The NBO charges of N bridge in **1**, **4** and **7** are -0.36285e, -0.54737e and -0.56883e; the NBO charges of O bridge in **2**, **5** and **8** are -0.45454e, -0.46470e and -0.47372e; the NBO charges of S bridge in **3**, **6** and **9** are 0.43772e, 0.40189e and 0.36804e, respectively. According to Allen electronegativity theory[39], the electronegativity values of C, N, O and S are 2.50, 3.07, 3.50 and 2.44 respectively. Therefore, the NBO charges of N and O atom are negative value; the NBO charge of S atom is positive value. Therefore, the embedded N atoms located in the 3,4-position of central spacer have stronger electron withdrawing effects to debase density of heterocyclic.

The shorter heteroatom-linked bridge NBO charge negative mobile made the electronic communication abated when molecules structure established by deliberately designed (Figure 5). The other atoms NBO charges in central spacer have no obvious relationship with electronic communication (Table S4). Hence, the electronic communication capacity was highly depend on shorter heteroatom-linked bridge NBO charge, this conclusion was consistent with our previous work[31], and the shorter heteroatom-linked bridge NBO charges was influenced by the molecules structure of central heterocyclic. This work revealed that the electrochemical interaction receded with increase the heteroatom number in central heterocycle spacer, and the electronic interaction could be artificial regulated by modified molecular structure of central heterocycle spacer.

In conclusion, nine 2,5-diferrocenyl five-membered derivatives have been discussed deeply as the systematic electrochemical model. The results revealed electronic interaction had non-significant relationship with the distance of bimetal, π-conjugation effect and aromaticity of the central heterocyclic. The N atoms located in the 3,4-position of center heterocyclic could severe regulate the electronic transfer between two ferrocenyl units, and the intramolecular electronic interaction receded with the increase of heteroatom in centre heterocycle spacer.

Methods

Materials

All operations were carried out in an atmosphere of purified argon. All solvents were dried and distilled according to standard procedures. The reactions were monitored by thin-layer chromatography (TLC). 2-bromoacetyl-ferrocene[40], 1,2-bis(ferrocenecarbonyl)hydrazine[41,42], ferrocenecarbonyl-hydrazine[43], N-(Ferrocenecarbonylmethyl)ferrocenecarboxamide[44], ferroceneamidine[45,46] and cyanoferrocene[47] were prepared according to literature methods, and the solvents were commercially available. The **1-3** synthetic method have been report in our previous work[31]. The **4-9** were synthesized through cyclization reaction and the schematic preparation procedure of compounds (Figure 6) and characterization data are summarized in synthetic methods.

Characterization methods.

Cyclic voltammetry was performed on a platinum disk electrode in a dichloromethane solution of **1**-**9** with tetra-n-butylammonium hexafluorophosphate [NBu_4] [PF_6] (0.1 M) as the supporting electrolyte, at a scan rate of 100 mV s^{-1}. The reference electrode was an Ag/Ag^+ electrode and the auxiliary electrode was a coiled platinum wire. Oxygen was purged from the one-compartment cell before each electrochemical run. The geometry optimizations and DFT calculations of **1**-**9** were undertaken using the B3LYP functional and 6-31G* basis set combination.

Synthetic methods.

2,5-diferrocenyl-1H-imidazole (**4**): Ferroceneamidine (120.1 mg, 0.53 mmol), 2-bromoacetyl-ferrocene (200.5 mg, 0.65 mmol), K_2CO_3 (75.1 mg, 0.57 mmol) and THF (25 ml) were added to a shrek reactor under atmosphere of pure argon stirred at 90 °C for 24 h. The reaction solution was cooled to room temperature, the solvent removed in vacuo, and the residue was subjected to chromatographic separation on a silica gel column (2.0×30 cm) using a mixture of dichloromethane/petroleum ether (1/1, v/v) to elute the product at room temperature. The first orange band was unreacted 2-bromoacetyl-ferrocene. The second orange band was compound **4** (120.2 mg). Yield: 27.5%, m.p. 218-220 °C. Anal. Calcd for $C_{23}H_{20}N_2Fe_2$: C, 63.34; H, 4.62; N, 6.42. Found: C, 63.77; H, 4.71; N, 7.01%. IR (KBr disk): 3083 cm^{-1} [Cp, v_{C-H}]; 1612 cm^{-1} [Cp, $v_{C=C}$]; 1432 cm^{-1} [$C_3H_2N_2$, $v_{N=C}$]; 1414 cm^{-1} [$C_3H_2N_2$, $v_{C=C}$]; 1104, 1000 cm^{-1} [Cp, δ_{C-H}]; 809 cm^{-1} [Cp, γ_{C-H}]. ^{1}H-NMR ($CDCl_3$, δ): 12.48 (s, 1H, $C_3H_2N_2$), 7.27 (s, 1H, $C_3H_2N_2$), 4.25-4.72 (m, 18H, Cp). ^{13}C-NMR ($CDCl_3$, δ): 161.32, 161.15 (C*i*-$C_3H_2N_2$), 117.39 ($C_3H_2N_2$), 77.26, 77.00, 76.75, 70.61, 70.45, 69.56, 69.35, 69.17, 68.05 (Cp). MS (ESI, relative abundance): 437.1 ($M+1^+$, 100%).

2,5-diferrocenyloxazole (**5**): *N*-(Ferrocenecarbonylmethyl)ferrocenecarboxamide (223.2 mg, 0.5 mmol) and pyridine (20 ml) were a shrek reactor in atmosphere of pure argon stirred at 0 °C for 0.5 h, then $POCl_3$ (0.5 ml, 5.0 mmol) was added to reactor stirred at room temperature (20 °C for 12 h. The reaction solution poured into crushed ice, then the solvent and the precipitate extracted by ethyl acetate (15 ml×3), and

then the organic phase removed in vacuo. And the residue was subjected to chromatographic separation on silica gel column (2.0×30 cm) using a mixture of dichloromethane/petroleum ether (1/1, v/v) to elute the product at room temperature. The first orange band was compound **5** (131.6 mg). Yield: 59.9%, m.p. 158-160 °C. Anal. Calcd for $C_{23}H_{20}NOFe_2$: C, 63.20; H, 4.38; N, 3.20. Found: C, 63.54; H, 4.11; N, 3.51%. IR (KBr disk): 3098 cm^{-1} [Cp, v_{C-H}]; 1613 cm^{-1} [Cp, $v_{C=C}$]; 1588 cm^{-1} [C_3HNO, $v_{N=C}$]; 1409 cm^{-1} [C_3HNO, $v_{C=C}$]; 1105, 1001 cm^{-1} [Cp, δ_{C-H}]; 815 cm^{-1} [Cp, γ_{C-H}]. ^{1}H-NMR ($CDCl_3$, δ): 6.94 (s, 1H, C_3HNO), 4.17-4.96 (m, 18H, Cp). ^{13}C-NMR ($CDCl_3$, δ): 162.18, 150.16 (C*i*-C_3HNO), 122.18 (C_3HNO), 77.29, 77.04, 76.78, 69.63, 69.28, 68.67, 67.77, 66.40, 66.38, 65.70 (Cp). MS (ESI, relative abundance): 437.1 (M^+, 100%).

2,5-diferrocenylthiazole (**6**): *N*-(Ferrocenecarbonylmethyl)ferrocenecarboxamide (222.8 mg, 0.5 mmol), lawessons reagent (244.1 mg, 0.6 mmol) and THF (20 ml) were added to a shrek reactor in atmosphere of pure argon stirred at 80 °C for 12h. The reaction solution was cooled to room temperature, then the solvent removed in vacuo, and the residue was subjected to chromatographic separation on silica gel column (2.0×30 cm) using a mixture of dichloromethane/petroleum ether (1/1, v/v) to elute the product at room temperature. The first orange band was compound **6** (177.0 mg). The single crystal of **6** was obtained through recrystallizing from hexane/dichloromethane (4/1, v/v) at low temperature (-15 °C). Yield: 78.1%, m.p. 221-223 °C. Anal. Calcd for $C_{23}H_{20}NSFe_2$: C, 60.96; H, 4.23; N, 3.09. Found: C, 59.54; H, 4.61; N, 3.52%. IR (KBr disk): 3090 cm^{-1} [Cp, v_{C-H}]; 1543 cm^{-1} [Cp, $v_{C=C}$]; 1470 cm^{-1} [C_3HNS, $v_{N=C}$]; 1259 cm^{-1} [C_3HNS, $v_{C=C}$]; 1104, 1029 cm^{-1} [Cp, δ_{C-H}]; 813 cm^{-1} [Cp, γ_{C-H}]. ^{1}H-NMR ($CDCl_3$, δ): 7.52 (m, 1H, C_3HNS), 4.14-4.88 (m, 18H, Cp). ^{13}C-NMR ($CDCl_3$, δ): 162.82, 136.51 (C*i*-C_3HNS), 137.59 (C_3HNS), 77.27, 77.02, 77.76, 71.22, 71.06, 70.25, 70.07, 69.96, 69.31, 68.74, 68.00, 66.72 (Cp). MS (ESI, relative abundance): 453.0 (M^+, 100%).

2,5-diferrocenyl-1,3,4-triazole (**7**): Cyanoferrocene (211.1 mg, 1.0 mmol), sodium methoxide (216.3 mg, 4.0 mmol) and methanol (20 ml) were added to a shrek reactor in atmosphere of pure argon stirred at 75 °C for 24 h, and then ferrocenecarbonyl-hydrazine (244.2 mg, 1.0 mmol) was added to reactor stirred at 75 °C for 24 h. The reaction solution was poured into crushed ice, then the solvent and the precipitate were extracted by ethyl acetate (25 ml×5), and then the organic phase was removed in vacuo. And the residue was subjected to chromatographic separation on silica gel column (2.0×20 cm) using a mixture of dichloromethane/petroleum ether (1/1, v/v) to elute the product at room temperature. The first yellow band was unreacted cyanoferrocene. The second orange band was compound **7** (301.2 mg). Yield: 68.8%, m.p. 194-196 °C Anal. Calcd for $C_{22}H_{19}N_3Fe_2$: C, 60.45; H, 4.38; N, 9.61. Found: C, 61.07; H, 4.79; N, 10.01%. IR (KBr disk): 3111 cm^{-1} [Cp, v_{C-H}]; 1648 cm^{-1} [Cp, $v_{C=C}$]; 1471 cm^{-1} [C_2HN_3, $v_{N=C}$]; 1104, 1025 cm^{-1} [Cp, δ_{C-H}]; 827 cm^{-1} [Cp, γ_{C-H}]. ^{1}H-NMR ($CDCl_3$, δ): 12.11 (s, 1H, C_2HN_3), 4.89-4.33 (m, 18H, Cp). ^{13}C-NMR ($CDCl_3$, δ): 173.58 (C*i*-C_2HN_2), 71.31, 71.82, 71.80, 71.19, 71.17, 70.99, 7.041, 70.09, 69.80, 69.70, 68.85 (Cp). MS (ESI, relative abundance): 437.1 (M^+, 100%).

2,5-diferrocenyl-1,3,4-oxadiazole (**8**): 1,2-bis(ferrocenecarbonyl)hydrazine (228.1 mg, 0.5 mmol) and pyridine (20 ml) were added to a shrek reactor in atmosphere of pure argon stirred at 0 °C for 0.5 h, then

$POCl_3$ (0.5 ml, 5.0 mmol) was added to reactor stirred at room temperature (20 °C) for 12 h. The reaction solution was poured into crushed ice, then the solvent and the precipitate were extracted by ethyl acetate (20 ml×3), and then the organic phase was removed in vacuo. And the residue was subjected to chromatographic separation on silica gel column (2.0×20 cm) using a mixture of dichloromethane/petroleum ether (1/1, v/v) to elute the product at room temperature. The first orange band was compound **8** (155.4 mg), and the single crystal of **8** was obtained through recrystallizing from hexane/dichloromethane (4/1, v/v) at low temperature (-15 °C). Yield: 70.7%, m.p. 216-219 °C. Anal. Calcd for $C_{22}H_{18}N_2OFe_2$: C, 60.32; H, 4.14; N, 6.39. Found: C, 60.64; H, 4.46; N, 6.77%. IR (KBr disk): 3111 cm^{-1} [Cp, ν_{C-H}]; 1604 cm^{-1} [Cp, $\nu_{C=C}$]; 1579 cm^{-1} [C_2N_2O, ν_{O-C}]; 1457 cm^{-1} [C_2N_2O, $\nu_{N=C}$]; 1104, 1025 cm^{-1} [Cp, δ_{C-H}]; 809 cm^{-1} [Cp, γ_{C-H}]. ^{1}H-NMR ($CDCl_3$, δ): 5.00-4.21 (m, 18H, Cp). ^{13}C-NMR ($CDCl_3$, δ): 165.97 (C*i*-C_2N_2O), 77.33, 77.08, 76.82, 70.70, 69.84, 67.97, 66.89 (Cp). MS (ESI, relative abundance): 438.0 (M^+, 100%).

2,5-diferrocenyl-1,3,4-thiadiazole (**9**): 1,2-bis(ferrocenecarbonyl)hydrazine (228.0 mg, 0.5 mmol), lawessons reagent (244.3 mg, 0.6 mmol) and THF (20 ml) were added to a shrek reactor under atmosphere of pure argon stirred at 80 °C for 12 h. The reaction solution was cooled to room temperature, then the solvent was removed in vacuo, and the residue was subjected to chromatographic separation on silica gel column (2.0×20 cm) using a mixture of dichloromethane/petroleum ether (1/1, v/v) to elute the product at room temperature.. The first orange band was compound **9** (189.0 mg). The single crystal of **9** was obtained through recrystallizing from hexane/dichloromethane (4/1, v/v) at low temperature (-15 °C). Yield: 83.2%, m.p. 206-212 °C Anal. Calcd for $C_{22}H_{18}N_2SFe_2$: C, 58.18; H, 3.99; N, 6.17. Found: C, 59.22; H, 4.22; N, 6.55%. IR (KBr disk): 3093 cm^{-1} [Cp, ν_{C-H}]; 1572 cm^{-1} [Cp, $\nu_{C=C}$]; 1518 cm^{-1} [C_2N_2S, ν_{S-C}]; 1410 cm^{-1} [C_2N_2S, $\nu_{N=C}$]; 1104, 1000 cm^{-1} [Cp, δ_{C-H}]; 820 cm^{-1} [Cp, γ_{C-H}]. ^{1}H-NMR ($CDCl_3$, δ): 5.00-4.18 (m, 18H, Cp). ^{13}C-NMR ($CDCl_3$, δ): 167.75, 165.95 (C*i*-C_2N_2S), 77.28, 77.03, 76.78, 74.08, 70.68, 70.58, 70.34, 69.82, 68.89, 67.96, 66.87 (Cp). MS (ESI, relative abundance): 454.0 (M^+, 100%).

Declarations

Acknowledgements (not compulsory)

We are grateful to the Natural Science Foundation of China (22065028), the Natural Science Foundation of Inner Mongolia (2017MS(LH)0202) and University Scientific research Foundation of Inner Mongolia (NJZY17102).

Author contributions statement

All authors reviewed the manuscript. Y.Q.H and L.M.H. conceived and designed the experiments. Y.Q.H and N.W. analyzed the data. Y.Q.H wrote the manuscript. Y.Q.H, L.M.H. and N.W. are involved in the related discussion. All authors reviewed the manuscript.

Competing Interests: The authors declare no competing interests.

Publisher's note: Springer Nature remains neutral with regard to jurisdictional claims in published maps and

institutional affiliations.

References

1. Ramandeep, K. et al. Understanding and Controlling Short- and Long-Range Electron/Charge-Transfer Processes in Electron Donor-Acceptor Conjugates. *Am. Chem. Soc.***142(17)**, 7898-7911, DOI: https://doi.org/10.1021/jacs.0c01452 (2020).
2. Albert, C. A. et al. Control over Near-Ballistic Electron Transport through Formation of Parallel Pathways in a Single-Molecule Wire. *Am. Chem. Soc*. **141(1)**, 240-250, DOI: https://doi.org/10.1021/jacs.8b09086 (2019).
3. Masayuki, N. Karin, S. et al. Intramolecular Electron Transfers in a Series of [Co_2Fe_2] Tetranuclear Complexes. *Chem.***58(18)**, 11912-11919, DOI: https://doi.org/10.1021/acs.inorgchem.9b00776 (2019).
4. Ke, Q. Shukkoor, M. K. Jian, L. et al. Carbohydrate-functionalized polythiophene biointerface: design, fabrication, characterization and application for protein analysis. *Applied Surface Science.***486**, 561-570, DOI: https://doi.org/10.1016/j.apsusc.2019.04.231 (2019).
5. Kristina, H. Christoph, F. Katja, H. Redox-Controlled Stabilization of an Open-Shell Intermediate in a Bioinspired Enzyme Model. *J. Inorg. Chem.***31**, 3537-3547, DOI: https://doi.org/10.1002/ejic.201800570 (2018).
6. My, P. T. C. Quail, J. W. et al. Enantiopure Ferrocenophanes with Phosphorus in Bridging Positions: Thermostability and Ring-Opening Polymerization. *Organometallics*. **38(9)**, 2092-2104, DOI: https://doi.org/10.1021/acs.organomet.9b00114 (2019).
7. Wang,Y. P. Lin, T. B. et al. 2D HETCOR NMR spectra and unequivocal assignments of (E)- and (Z)-1-ferrocenyl-2-phenylethene, and (1E,3E)- and (1Z,3E)-1-ferrocenyl-4-phenyl-1,3-butadiene, (E)-1,2-diferreocenylethene, and (1E,3E)-1,4-diferrocenyl-1,3-butadiene in ^{13}C NMR spectra. *Polyhedron*. **127**, 410-419, DOI: https://doi.org/10.1016/j.poly.2016.10.006 (2017).
8. Ma, J. X. Nico, K. et al. 1,1'-Dialkynylferrocenes as Substrates for Bidirectional Alkyne Metathesis Reaction. *J. Org. Chem*. **20**, 4510-4518, DOI: https://doi.org/10.1002/ejoc.201500483 (2015).
9. Peng, H. Baokang, J. et al. Synthesis, electrochemistry and IR spectroelectrochemistry of bisferrocenyl bridged benzene derivates. *Journal of Organometallic Chemistry*. **697**, 57-64, DOI: https://doi.org/10.1016/j.jorganchem.2011.10.019 (2012).
10. Eric, G. Bertrand, G. et al. Intramolecular Electron Transfers Thwart Bistability in a Pentanuclear Iron Complex. *Inorganic Chemistry*. **55(18)**, 9178-9186, DOI: https://doi.org/10.1021/acs.inorgchem.6b00791 (2016).

11. Han, W. X. Shi, Y. Z. et al. Synthesis and electrochemical, linear and third-order nonlinear optical properties of ferrocene-based D-π-A dyes as novel photoredox catalysts in photopolymerization under visible LED irradiations. *Dyes and Pigments*. **166**, 140-148, DOI: https://doi.org/10.1016/j.dyepig.2019.03.023 (2019).
12. Rani, A. Michal, V. et al. Real-Time Detection of Redox Events in Molecular Junctions. *Am. Chem. Soc*. **136(6)**, 2674-2680, DOI: https://doi.org/10.1021/ja412668f (2014).
13. Xie, R. J. Han, L. M. et al. Molecular structure and electrochemistry of carbon-bridged diferrocenyl compounds. *Coord. Chem*. **63(10)**, 1700-1710, DOI: https://doi.org/10.1080/00958972.2010.487102 (2010).
14. Julio, A. Angel, E. K. Structural and pH Control on the Electronic Communication between Two Identical Ferrocene Sites. *Organometallics*. **18(26)**, 5733-5734, DOI: https://doi.org/10.1021/om990678r (1999).
15. Alessandro, D. Annalisa, B. et al. Electron transfer within C_4 unsaturated spacers between terminal ferrocenyl moieties. *Inorganica Chimica Acta*. **374(1)**, 442-446, DOI: https://doi.org/10.1016/j.ica.2011.03.014 (2011).
16. Victor, N. N. Semyon, V. D. et al. Probing Electronic Communications in Heterotrinuclear Fe-Ru-Fe Molecular Wires Formed by Ruthenium(II) Tetraphenylporphyrin and Isocyanoferrocene or 1,1'-Diisocyanoferrocene Ligands. *Chem*. **54(22)**, 10711-10724, DOI: https://doi.org/10.1021/acs.inorgchem.5b01614 (2015).
17. John, R. H. Yu, J. X. et al. Unraveling the Interplay of Backbone Rigidity and Electron Rich Side-Chains on Electron Transfer in Peptides: The Realization of Tunable Molecular Wires. *Am. Chem. Soc*. **136(35)**, 12479-12488, DOI: https://doi.org/10.1021/ja507175b (2014).
18. Yu, J. X. John, R. H. The effect of a macrocyclic constraint on electron transfer in helical peptides: A step towards tunable molecular wires. *Commun*. **50**, 1652-1654, DOI: https://doi.org/10.1039/c3cc47885h (2014).
19. Alexander, H. Dieter, S. et al. Diferrocenes containing thiadiazole connectivities. *Inorganica Chimica Acta*. **374**, 112-118, DOI: https://doi.org/10.1016/j.ica.2011.02.058 (2011).
20. Wang, Y. Q. Han, L. M. et al. Synthesis, structure and electrochemistry of new diferrocenyl pyridine derivatives. *Polyhedron*. **54**, 221-227, DOI: https://doi.org/10.1016/j.poly.2013.02.043 (2013).
21. Huang, C. B. Huang, Y. F. et al. Cycloheptyl-fused N,N,N'-chromium catalysts with selectivity for vinyl-terminated polyethylene waxes: thermal optimization and polymer functionalization. *Dalton Trans*. **47**, 13487-13497, DOI: https://doi.org/10.1039/C8DT03052A (2018).
22. Cendrine, P. Christophe, C. et al. Topological Effects on Intramolecular Electron Transfer via Quantum Interference. *Chem*. **36(22)**, 5037-5049, DOI: https://doi.org/10.1021/ic970013m (1997).
23. Rajneesh, M. Rekha, S. et al. Star shaped ferrocenyl truxenes: synthesis, structure and properties. *Dalton Trans*. **43**, 6891-6896, DOI: https://doi.org/10.1039/C4DT00210E (2014).
24. James, R. W. Karl, J. S. et al. 3,5-Diferrocenylpyridine: Synthesis, characterisation, palladium(II) dichloride complex and electrochemistry. *Polyhedron*. **36**, 73-78, DOI:

https://doi.org/10.1016/j.poly.2012.01.028 (2012).

25. Ritu, S. Dhara, P. et al. A mini review: recent developments of heterocyclic chemistry in some drug discovery scaffolds synthesis. *Journal of Medicinal and Chemical Sciences*. **3(1)**, 71-78, DOI: 26655/JMCHEMSCI.2020.1.9 (2020).
26. Tauchman, J. Jakub, T. et al. Synthesis, crystal structures and electrochemistry of ferrocenyl-substituted 1,3,4-oxadiazoles. *Czech. Chem. Commun*. **75**, 1023-1040, DOI: 10.1135/cccc2010064 (2010).
27. Liu, Z. S. Zhu, N. et al. Detecting the electron density of benzene using ferrocene as an indicator. *Coord. Chem*. **65(16)**, 2804-2810, DOI: https://doi.org/10.1080/00958972.2012.704024 (2012).
28. Xie, R. J. Han, L. M. et al. An effective method for the synthesis of monoferrocenylbenzene derivatives. *Coord. Chem*. **65(23)**, 4086-4095, DOI: https://doi.org/10.1080/00958972.2012.732696 (2012).
29. Xie, R. J. Han, L. M. et al. The effect of acetyl on the electronic communication of carbon-bridged diferrocene. *Coord. Chem*. **64(18)**, 3180-3188, DOI: https://doi.org/10.1080/00958972.2011.616198 (2011).
30. Xie, R. J. Han, L. M. et al. Synthesis of ortho-diferrocenylbenzene with cobalt clusters as reaction precursors: Crystal structure and electrochemical properties. *Polyhedron*. **38(1)**, 7-14, DOI: https://doi.org/10.1016/j.poly.2012.02.018 (2012).
31. Hu, Y. Q. Han, L. M. et al. Synthesis of 2,5-diferrocenyl five-membered heterocyclic compounds and their electrochemistry. *Coord. Chem*. **66(19)**, 3481-3497, DOI: https://doi.org/10.1080/00958972.2013.841902 (2013).
32. Hu, Y. Q. Zhu, N. et al. Channel of Electronic Interactions in Diferrocenyl Pyrrole Derivatives. *Acta Physico-Chimica Sinica*. **31(2)**, 227-236, DOI: 3866/PKU.WHXB201411061 (2015).
33. Alexander, H. Dieter, S. et al. Diferrocenes containing thiadiazole connectivities. *Inorganica Chimica Acta*. **374(1)**, 112-118, DOI: https://doi.org/10.1016/j.ica.2011.02.058 (2011).
34. Smith, M. B. March, J. *March's Advanced Organic Chemistry*. **2**, 54, DOI: https://doi.org/10.1002/9780470084960.ch2 (2007).
35. Luo, M. H. Han, L. M. et al. Synthesis and structural characterization of ferrocenyl indenyl derivatives. *Coord. Chem*. **63(21)**, 3805-3815, DOI: https://doi.org/10.1080/00958972.2010.521937 (2010).
36. Cendrine, P. Christophe, C. et al. Topological Effects on Intramolecular Electron Transfer via Quantum Interference. *Inorganic Chemistry*. **36(22)**, 5037-5049, DOI: https://doi.org/10.1021/ic970013m (1997).
37. Chemical Bonding and Aromaticity in Furan, Pyrrole, and Thiophene: A Magnetic Shielding Study. *Journal of Organic Chemistry*. **78(16)**, 8037-8043, DOI: https://doi.org/10.1021/jo401319k (2013).
38. Kate, E. H. Peter, B. K. Shielding in and around Oxazole, Imidazole, and Thiazole: How Does the Second Heteroatom Affect Aromaticity and Bonding? *Journal of Organic Chemistry*. **80(14)**, 7150-7157, DOI: https://doi.org/10.1021/acs.joc.5b01010 (2015).

39. Leland, C. A. Electronegativity is the average one-electron energy of the valence-shell electrons in ground-state free atoms. *Journal of the American Chemical Society*. **111(25)**, 9003-9014, DOI: https://doi.org/10.1021/ja00207a003 (1989).
40. Alberto, T. Pedro, M. et al. Aza-wittig reactions of iminophosphoranes derived from ferrocenylazido ketones: preparation and electrochemical study of novel ferrocenyl-substituted azaheterocycles. *Tetrahedron*. **55(51)**, 14701-14718, DOI: https://doi.org/10.1016/S0040-4020(99)00916-3 (1999).
41. Raspopova, E. A. Popov, L. D. et al. Synthesis, structure, and complexing ability of pyrrole-2-carbaldehyde ferrocenoylhydrazone. *Russian Journal of General Chemistry*. **78(8)**, 1586-1593, DOI: https://doi.org/10.1134/S1070363208080215 (2008).
42. Gabin, M. M. Jouda, J. et al. Synthesis and antimycobacterial activity of a series of ferrocenyl derivatives. *European Journal of Medicinal Chemistry*. **46(1)**, 31-38, DOI: https://doi.org/10.1016/j.ejmech.2010.10.004 (2010).
43. Petr, S. Ivana, C. et al. The crystal structures, molecular spectra and thermal behaviour of carbamoylferrocene and ferrocenecarbonylhydrazide. *Polyhedron*. **29(1)**, 134-141, DOI: https://doi.org/10.1016/j.poly.2009.06.034 (2010).
44. Alberto, T. Pedro, M. et al. Synthesis of the first homobimetallic thiazole–ferrocene ligand displaying metal–metal interaction and redox-switchable proton affinity. *Tetrahedron Letters*. **43(47)**, 8453-8457, DOI: https://doi.org/10.1016/S0040-4039(02)02097-X (2002).
45. Zhang, P. T. Yang, X. Y. et al. Pyridinylpyrimidines selectively inhibit human methionine aminopeptidase-1. *Bioorganic & Medicinal Chemistry*. **21(9)**, 2600-2617, DOI: https://doi.org/10.1016/j.bmc.2013.02.023 (2013).
46. Omid, K. A. Nader, S. et al. Synthesis of a series of carbon-14 labeled tetrahydropyrido[4,3-d]pyrimidin-4(3H)-ones. *Journal of Labelled Compounds and Radiopharmaceuticals*. **56(14)**, 722-725, DOI: https://doi.org/10.1002/jlcr.3110 (2013).
47. Ma, J. Cui, X. L. et al. Ferrocenylimidazoline palladacycles: efficient phosphine-free catalysts for Suzuki-Miyaura cross-

Figures

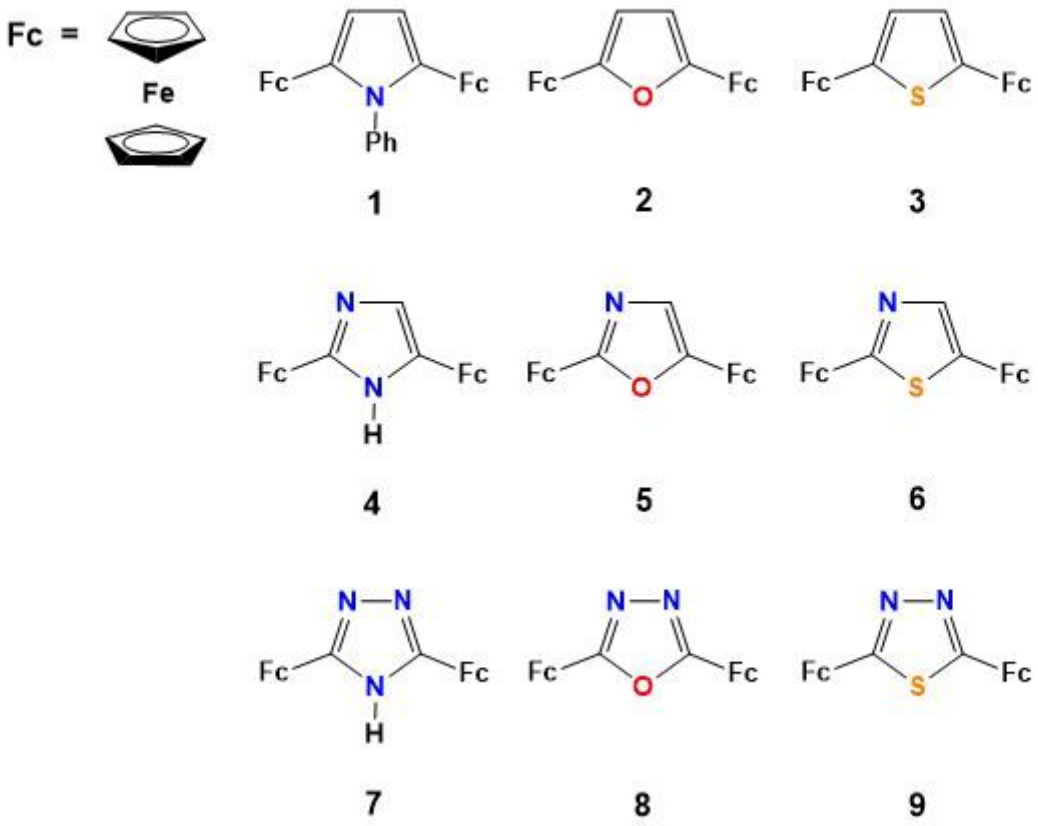

Figure 1

The structural formulas of 1-9

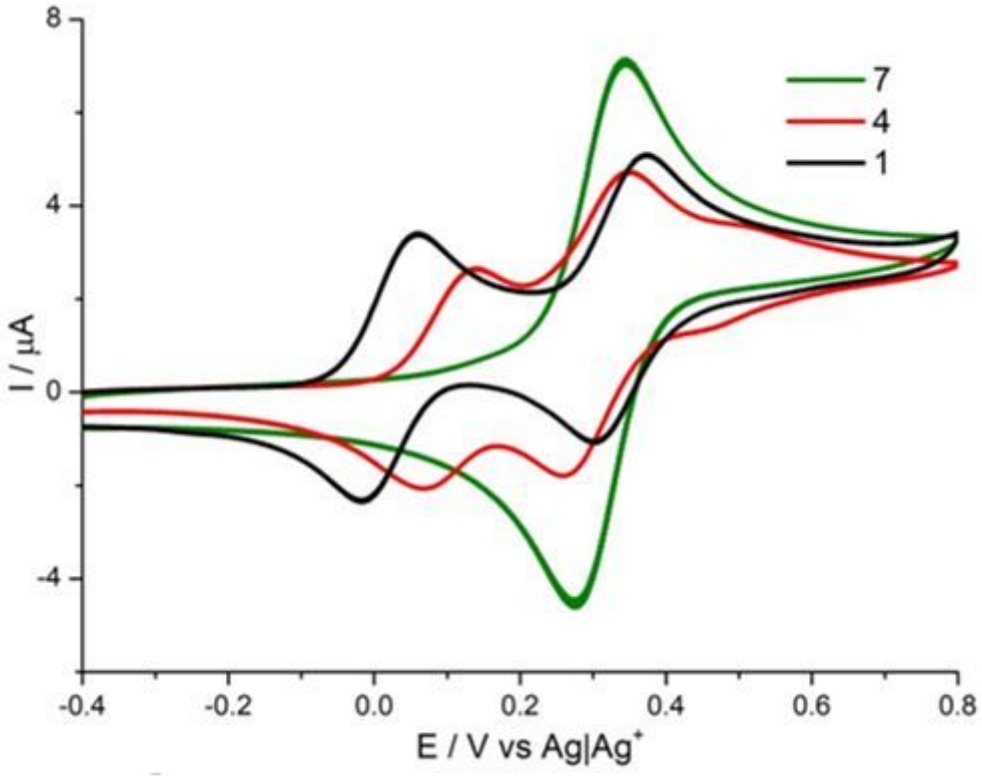

Figure 2

The cyclic voltammograms of 1, 4 and 7

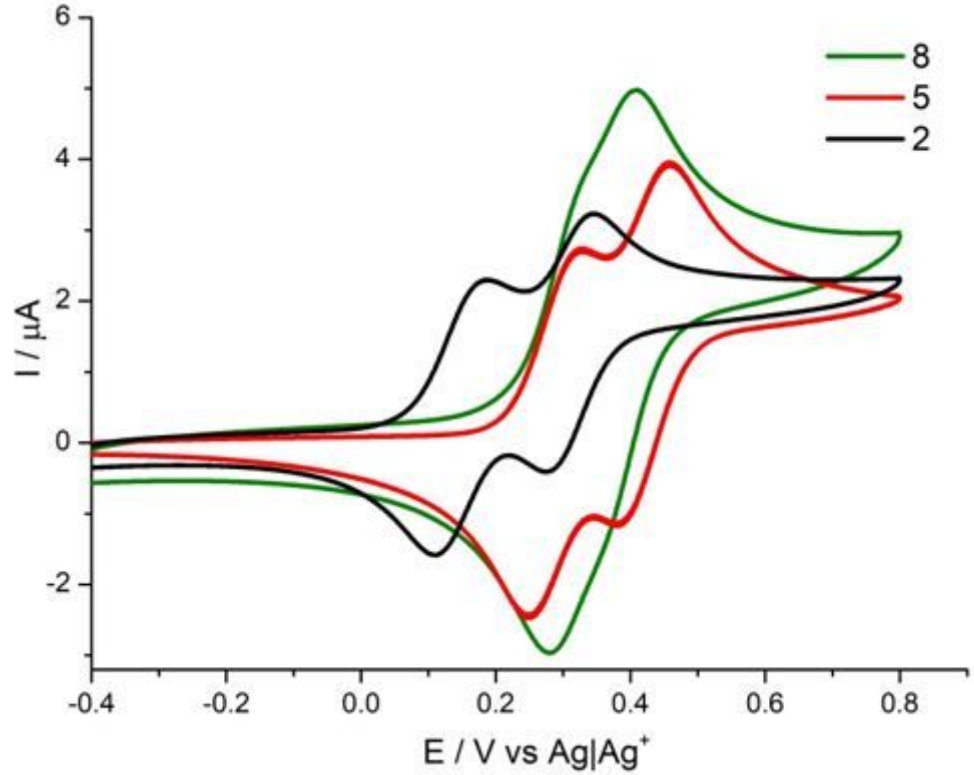

Figure 3

The cyclic voltammograms of 2, 5 and 8

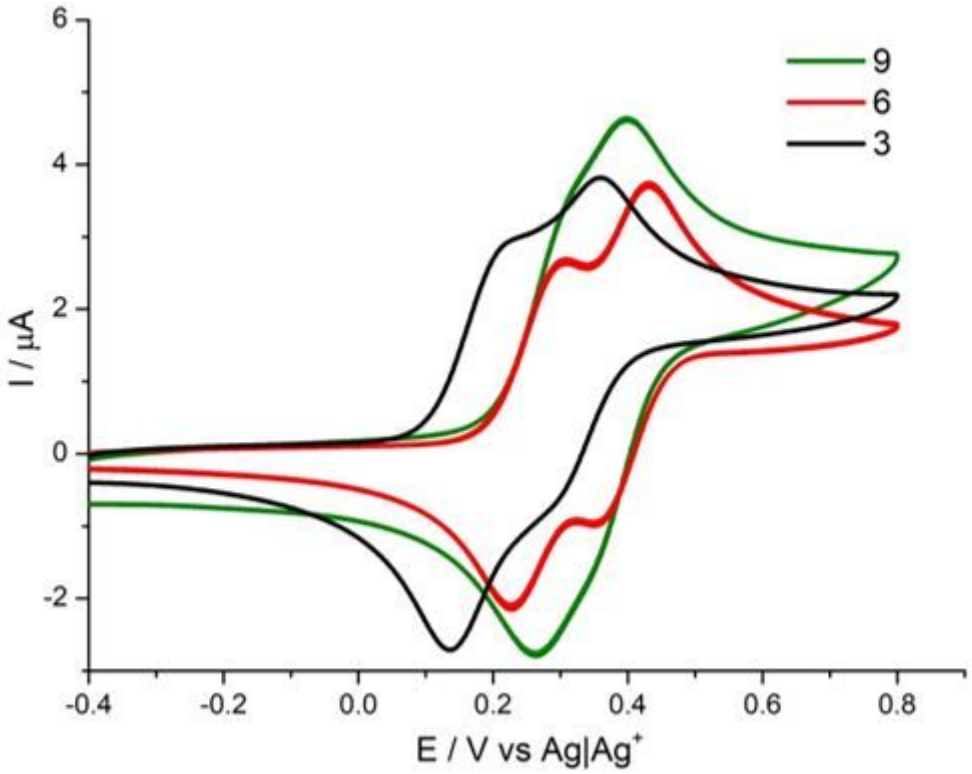

Figure 4

The cyclic voltammograms of 3, 6 and 9

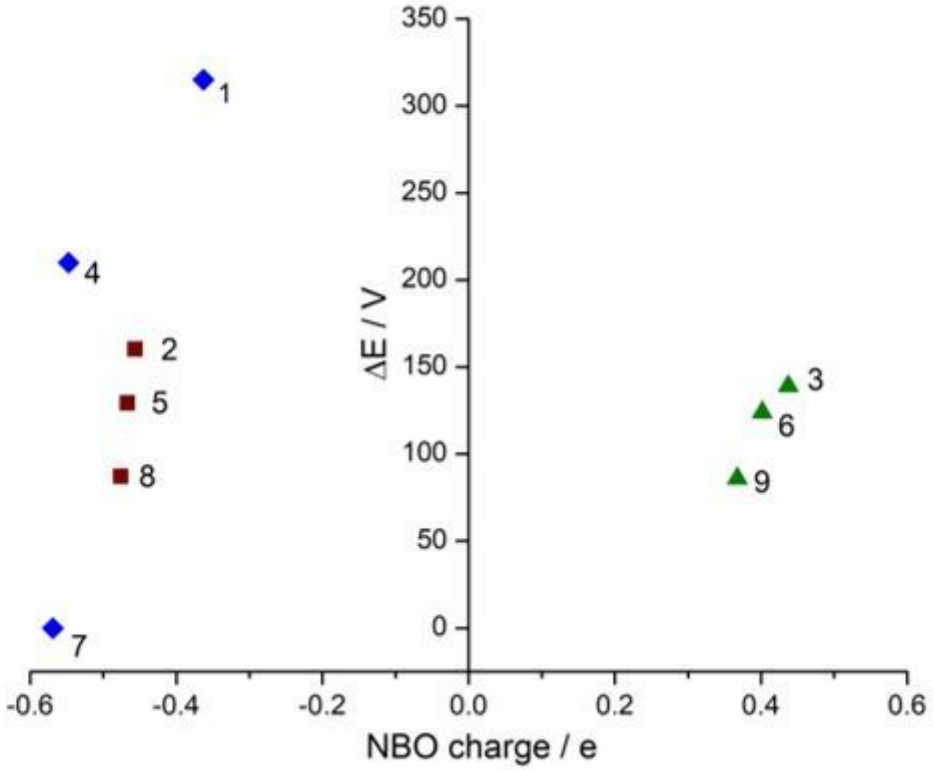

Figure 5

The relationship of shorter heteroatom-linked bridge NBO charge with electronic communication of 1-9

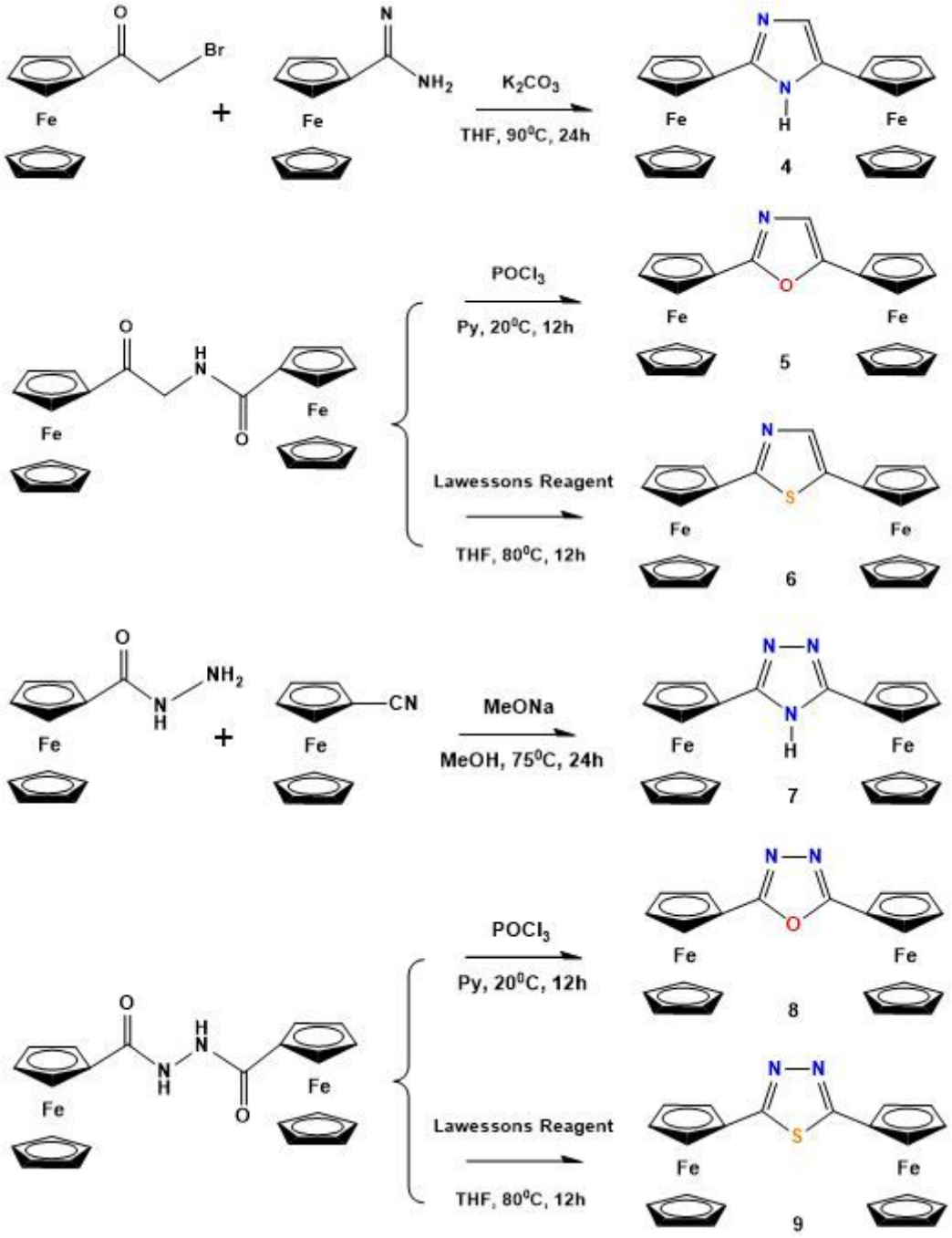

Figure 6

The schematic preparation procedure of compounds

Supplementary Files

This is a list of supplementary files associated with this preprint. Click to download.

- SupportingInformation.docx